ORIGINAL RESEARCH

Seasonal variability of phytoplankton community structure in a coastal station of the Argentine continental shelf based on a chemotaxonomic approach

M. Guillermina Ruiz*, M. Belén Mattera Coy, Mario C. Carignan, Macarena Albornoz, Graciela N. Molinari and Nora G. Montoya

[1]Instituto Nacional de Investigación y Desarrollo Pesquero (INIDEP), Paseo Victoria Ocampo Nº 1, Escollera Norte, B7602HSA - Mar del Plata, Argentina. ORCID *M. Guillermina Ruiz* https://orcid.org/0000-0003-0242-4846, *M. Belén Mattera Coy* https://orcid.org/0000-0001-6170-6902, *Macarena Albornoz* https://orcid.org/0009-0002-6240-744X, *Graciela N. Molinari* https://orcid.org/0009-0008-3671-5071, *Nora G. Montoya* https://orcid.org/0009-0000-2274-5001

Marine and Fishery Sciences MAFIS

ABSTRACT. The composition, abundance and size structure of the phytoplankton community at a coastal time series station (38° 28′ S-57° 41′ W, EPEA, Argentina) was characterized by applying the chemotaxonomic approach. The seasonal variability of pigment diversity determined by high-performance liquid chromatography (HPLC, n = 171), nutrient concentration (n = 934), and temperature, salinity and degree of stratification of the water column was identified (n = 190 CTD profiles). The CHEMTAX program was used to estimate phytoplankton abundance in terms of contribution to chlorophyll *a* concentration of the different phytoplankton pigmentary types (PPTs). Two different pigment indices were compared to estimate phytoplankton community size fractions throughout the year, giving contrasting results. Water column was mostly mixed, with minimum temperatures between July and September and maximum between January-March (range: 8-23 °C). Nitrate was the limiting nutrient, with minimal concentrations at the end of summer. It's range varied between 0.010-13.330 µM, while silicate ranged between 0.016-10.670 µM without major seasonal variations, and phosphate between 0.120-2.180 µM. Fucoxanthin, chlorophyll *c*2, 19'-hexanoyl-oxy-fucoxanthin, diadinoxanthin, chlorophyll *b*, chlorophyll *c*3, peridinin and, alloxanthin, were the most frequent phytoplankton pigments. The PPT DINO-1 (dinoflagellates with peridinin), haptophytes types: HAPTO-6, HAPTO-7 and HAPTO-P showed a seasonal cycle with peaks of abundance in autumn and spring, while the diatoms DIATO-1 was high during the whole year and DIATO-2 mainly during winter. A pigment profile of a group of prymnesiophytes possessing MVChl_c3 was described. It was evident that at this site PPTs having potentially toxic species bloom under different hydrological conditions. DINO-1 is likely to bloom in April (autumn), with temperatures close to 18 °C and weak stratification conditions, while October bloom (spring) occurs with lower temperatures of 10-12 °C. DINO-4 was noted during January and February (summer), when temperature was > 18 °C, salinity < 33.7, and the water column showed maximum stratification. In contrast, the maximum abundances of DIATO-2 occurred between August and September (winter), under completely mixed conditions, high nitrate concentration and low temperature of 10 °C. This work constitutes the first description of the variability of the abundance of the main PPTs in a coastal a time series station in the southwestern Atlantic Ocean shelf throughout the annual cycle, demonstrating the power of chemotaxonomy and CHEMTAX to perform descriptive analysis of a large number of samples.

Key words: CHEMTAX, phytoplankton pigments, nutrients, dinoflagellates, harmful algal blooms, southwestern Atlantic.

*Correspondence:
mgruiz@inidep.edu.ar

Received: 2 May 2024
Accepted: 8 August 2024

ISSN 2683-7595 (print)
ISSN 2683-7951 (online)

https://ojs.inidep.edu.ar

Journal of the Instituto Nacional de Investigación y Desarrollo Pesquero (INIDEP)

Variabilidad estacional de la estructura de la comunidad fitoplanctónica en una estación costera de la plataforma continental argentina basada en un enfoque quimiotaxonómico

RESUMEN. Se caracterizó la composición, abundancia y estructura de tamaño de la comunidad fitoplanctónica en una estación costera (38° 28′S-57° 41′W, EPEA, Argentina) de serie de tiempo aplicando el enfoque quimiotaxonómico. Se identificó la variabilidad estacional de la diversidad de pigmentos determinada por cromatografía líquida de alta resolución (HPLC, n = 171), la concentración de nutrientes (n = 934) y la temperatura, salinidad y grado de estratificación de la columna de agua (n = 190 perfiles CTD). Se utilizó el programa CHEMTAX para estimar la abundancia de fitoplancton en términos de contribución a la concentración de clorofila *a* de los diferentes tipos pigmentarios de fitoplancton (PPTs). Se compararon dos índices pigmentarios diferentes para estimar las fracciones de tamaño de la comunidad fitoplanctónica a lo largo del año, obteniéndose resultados contrastantes. La columna de agua estuvo mayoritariamente mezclada, con temperaturas mínimas entre julio y septiembre, y máximas entre enero y marzo (rango: 8-23 °C). El nitrato fue el nutriente limitante, con concentraciones mínimas al final del verano. Su rango varió entre 0.010-13.330 μM, mientras que el silicato varió entre 0.016-10.670 μM sin grandes variaciones estacionales, y el fosfato entre 0.120-2.180 μM. La fucoxantina, clorofila *c*2, 19'-hexanoil-oxi-fucoxantina, diadinoxantina, clorofila *b*, clorofila *c*3, peridinina y aloxantina fueron los pigmentos fitoplanctónicos más frecuentes. Los PPT DINO-1 (dinoflagelados con peridinina), y los tipos de haptofitas HAPTO-6, HAPTO-7 y HAPTO-P mostraron un ciclo estacional con picos de abundancia en otoño y primavera, mientras que la abundancia de diatomeas DIATO-1 fue alta durante todo el año, y las DIATO-2 principalmente durante el invierno. Se describió un perfil de pigmentos de un grupo de primnesiófitas que poseen MVChl_c3. Se evidenció que en este sitio los PPTs que tienen especies potencialmente tóxicas florecen bajo diferentes condiciones hidrológicas. Es probable que DINO-1 florezca en abril (otoño) con temperaturas cercanas a 18 °C y condiciones de estratificación débil, mientras que la floración de octubre (primavera) ocurre con temperaturas más bajas de 10-12 °C. DINO-4 se observó durante enero y febrero (verano), cuando la temperatura fue > 18 °C, la salinidad < 33,7 y la columna de agua mostró una estratificación máxima. En cambio, las máximas abundancias de DIATO-2 se dieron entre agosto y septiembre (invierno), en condiciones de mezcla completa, alta concentración de nitratos y baja temperatura de 10 °C. Este trabajo constituye la primera descripción de la variabilidad de la abundancia de los principales PPTs en una estación de series de tiempo costera en la plataforma del Atlántico Sudoccidental a lo largo del ciclo anual, demostrando el poder de la quimiotaxonomía y CHEMTAX para realizar análisis descriptivos de un gran número de muestras.

Palabras clave: CHEMTAX, pigmentos fitoplanctónicos, nutrientes, dinoflagelados, floraciones algales nocivas, Atlántico Sudoccidental.

INTRODUCTION

The composition of phytoplankton communities varies in time and space, spanning several taxa and orders of magnitude in cell size (Jeffrey et al. 2011). Knowing the size structure of the phytoplankton community is key to understanding the dynamics of marine food webs or oceanic processes such as carbon flow or nutrient cycling (Bouman et al. 2005; Cai et al. 2019). At the same time, knowing the succession of species that make up the community is relevant, since different taxa have toxin-producing species representing a potential danger to marine fauna, fishery resources and public health (Montoya et al. 2018; Montoya 2019; Cadaillón et al. 2024).

The concentration of chlorophyll *a* (Chl_a) in seawater is the most used indicator of phytoplankton biomass, although it does not provide information on the community composition. On the other hand, chemotaxonomy based on the separation, identification and quantification of phytoplankton pigments diversity by high performance liquid chromatography (HPLC) is a powerful tool to study phytoplankton communities with high precision and reproducibility, overcoming some of the limitations of microscopy (e.g. underestimation of taxa not resistant to fixation or lacking identifying traits or the inability to identify cells smaller than 5 μm).

The theoretical foundation of chemotaxonomy is the existence of marker pigments assignable to different taxonomic levels (Jeffrey et al. 1997). Marker pigments have a restricted distribution to

an algal class, such as the carotenoid peridinin to a certain group of dinoflagellates, although in general it is a combination of pigments establishing the marker capacity. Therefore, pigment assemblages together with their typical relative concentrations allow the definition of different 'phytoplankton pigmentary types' (PPTs) and their applicability of pigment diversity to the study of phytoplankton taxonomy. Based on these principles, Mackey et al. (1996) developed 'CHEMTAX', a factor analysis to determine the relative abundance of different PPTs present in a set of samples. This analysis requires hypotheses about which PPTs are present in the samples and prior knowledge of the pigment:Chl_a ratios of their marker pigments. The CHEMTAX has been widely used in different environments such as the Southern Ocean (Rodríguez et al. 2002), Pacific waters (Armbrecht et al. 2015; Larios-Muñiz et al. 2022) and the Atlantic Ocean (Carreto et al. 2003, 2008, 2016, 2018; Goela et al. 2015; Nunes et al. 2019), revealing the structure of the phytoplankton community with a qualitative and quantitative approach.

In parallel, marker pigments can be used to determine the size structure of the phytoplankton community. Considering that some taxa are represented mostly in one of the three size classes (picoplankton < 2 μm, nanoplankton 2-20 μm and microplankton > 20 μm) proposed by Sieburth et al. (1978), Vidussi et al. (2001) proposed a method to estimate the relative proportion of these three classes based on 7 diagnostic pigments (DPs). Later, Uitz et al. (2006) modified Vidussi equations by applying weighted coefficients to the same DPs, obtaining equations to calculate the contribution to the total Chl_a concentration of each size class in a given sample. The 'Uitz indices' have been used in numerous studies and have been precursors of other similar indices applicable at a regional scale (Hirata et al. 2008; Brewin et al. 2010; Devred et al. 2011). Recently, Chase et al. (2020) proposed new equations using the same DPs but revising assumptions and reducing uncertainty in assigning PPTs to size classes, using flow cytometry for this purpose.

First studies aimed at understanding the plankton community and ecological conditions on the Argentine continental shelf, more precisely on the coast of the province of Buenos Aires, date back to the 1970s (Carreto et al. 1973) or even to some previous taxonomic studies. Thus, the dominance, from west to east, of microflagellates, diatoms and haptophytes was documented in a section in front of Mar del Plata city as the influence of Malvinas Current on the platform increases (Lange 1985). Studies on the abundance and distribution of toxic dinoflagellates gained greater importance in the region after the first toxic outbreak of paralytic shelfish poisoning (PSP) detected in the Argentine sea during the spring of 1980, causing the death of two fishermen due to ingestion of poisoned mussels (Carreto et al. 1981). At that time, a monitoring plan was established at a fixed station off Mar del Plata with the objective of investigating the levels of PSP toxicity in mussel (*Mytilus edulis*) populations as well as the relative abundance of the dinoflagellate *Alexandrium tamarense/catenella* complex. Towards the late 1990s, the mussel bank off Mar del Plata disappeared, but periodic sampling continued at the same site, capitalizing on the time series of previous ecological observations. The time series project was renamed and has been known as Estación Permanente de Estudios Ambientales (EPEA) since 2000. The EPEA station is located in the transition zone between the coastal and shelf systems on the Argentine continental shelf. Previous studies have partially reported the environmental characteristics of this fixed station (Carreto et al. 2004; Lutz et al. 2006; Viñas et al. 2013; Ruiz 2018; Ruiz et al. 2020), as well as the summer succession of pico and ultraphytoplankton (fraction between 2 and 5 μm) (Silva et al. 2009; Silva 2011). Under certain circumstances, harmful algal blooms (HABs) occur on the coast of the Argentine province of Buenos Aires, particularly species that produce paralytic, amnesic, and diarrheic shellfish toxins (Carreto et al. 2004; Fabro et al. 2017; Montoya et al. 2020). In this region, the increase in intensity and geographical spread

of blooms of *A. tamarense*/*catenella* complex and *Gymnodinium catenatum*, both species associated with PSP, have been documented (Méndez and Carreto 2018; Montoya et al. 2018). In addition, diarrheic toxins from shellfish associated with *Dinophysis* sp. have been recorded in Villa Gesell, Buenos Aires province (Montoya et al. 2008, 2020; Sar et al. 2012) and in Uruguay (Méndez and Medina 2004; Méndez and Carreto 2018), causing bans on the extraction and marketing of bivalves. Furthermore, amnesic shellfish toxins have been produced by some toxic diatoms of the genus *Pseudo-nitzschia* in the same region (Krock et al. 2018; Méndez and Carreto 2018; Montoya et al. 2020).

In this work, the annual cycle of hydrological conditions and the composition, abundance and size structure of the phytoplankton community were characterized applying the chemotaxonomic approach (pigment diversity and CHEMTAX) at this fixed station of ecological observations on the Argentine continental shelf. Main environmental factors driving the seasonal succession of different phytoplankton groups were discussed, with emphasis on dinoflagellates and diatom groups having toxigenic species.

MATERIALS AND METHODS

Sampling at the study site

The study site (EPEA, 38° 28′ S-57° 41′ W) is located at 13 nmi from the coast, in the proximity of the 50 m isobath (Figure 1). Periodic sampling began in 1994 and, from 2000 onwards, studies were expanded with the incorporation of new variables such as the diversity of phytoplankton pigments, among others. Typically, water sampling was performed with 4-liter Niskin bottles associated with a CTD/carousel water sampler system at discrete depths. Sampling depths were 0 m, 5 m, the depth of maximum fluorescence, and a depth below it just near the bottom. Data from the CTD were processed, qualified and incorporated into the BaRDO Regional Oceanographic Data Base of INIDEP (Instituto Nacional de Investigación y Desarrollo Pesquero) (BaRDO 2023) in order to obtain profiles of temperature, salinity and the Simpson parameter (Phi, φ) (Simpson et al. 1981). This parameter was used as a measure equivalent to the variation of the potential energy required to mix the water column, and used as an indicator of the degree of water column stratification. Given the large number of records representative of the entire annual cycle, Simpson values under the first quartile (Q1) were considered vertically homogeneous and values over the third quartile (Q3) were considered stratified waters.

Determination of nutrient concentration

The macronutrients nitrate, nitrite, phosphate and silicate were analyzed using two different autoanalyzers: autoAnalyzer II Technicon (years 1994-2018) and SKALAR San++ (year 2019). The method used for the analysis of nitrate and nitrite corresponded to a modification of the original method of Armstrong et al. (1967) (Skalar Methods, Catnr. 461-032). Phosphate was determined by a modification of the original procedure of Murphy and Riley (1962) (Skalar Methods, Catnr. 503-010w/r), while silicate analysis followed the method described by Grasshoff et al. (1983) (Skalar Methods, Catnr. 563-051). Since 2013, concentration calculations have been done using Certified Reference Material (CRM), manufactured by Kanso Technos Co., Ltd., Katano, Osaka, Japan 3.

Determination of the concentration of phytoplankton pigments by HPLC

A total of 171 samples from different depths (0-47 m) were analyzed in the period 2000-2005 (n = 64) and 2012-2019 (n = 107). The method of Garrido and Zapata (1997) was used for samples from 2000 to 2001, while the method of Zapata et al. (2000) was used for samples from 2002

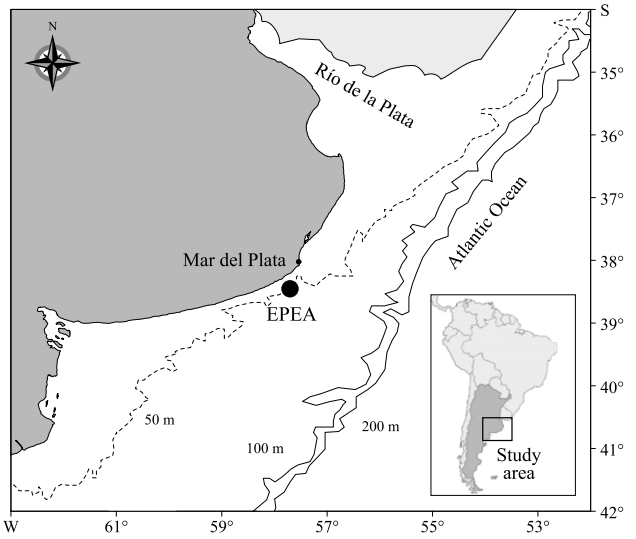

Figure 1. Study location. Former 'Estación de Marea Roja' currently known as 'Estación Permanente de Estudios Ambientales (EPEA)', 38° 28′S-57° 41′W.

onwards. Both methods were proved to resolve and separate chlorophyll *c*1, chlorophyll *c*2 and Mg-3,8-divinil-pheoporphyrin a5 mono-methyl ester (MgDVP). The chromatographic method was changed after the improvement that the authors made on their previous one, since the later provides a better resolution of the divinyl and monovinyl forms of chlorophyll *a* in natural sea water samples. However, at this study site there *Prochloroccocus marinus* was not present and therefore divinyl chlorophyll *a* was never detected (sea Results section, Table 3). Filters were kept in liquid nitrogen or ultra-freezer until being analyzed by HPLC. For pigments quantification, high purity standards acquired from the VKI (The International Agency for 14C Determination, Denmark) or isolated from cultures of *Emiliania huxleyi* (Haptophyta) clone CCMP 370 and the dinoflagellate *A. tamarense*/*catenella* complex clone MDQ 1096 were used. Those detected pigments for which the extinction coefficients were not known were quantified using the extinction coefficients of pigments containing the chromophore with the greatest similarity (e.g. chlorophyll *c*3 and non-polar chlorophylls *c* were quantified as chlorophyll equivalents *c*2).

Chemotaxonomic analysis of the phytoplankton community (CHEMTAX)

The CHEMTAX program version 1.95 based on Microsoft Excel provided by the Australian Antarctic Data Center (https://data.aad.gov.au) was used. This program allowed firstly to optimize the pigment:Chl_a ratios selected for the given set of samples, and secondly, to determine the biomass of each PPT as the proportion of Chl_a concentration contributed to the sample. Samples with Chl_a < 0.3 mgm^{-3} were excluded from the analysis since very low pigment concentration values increase the estimated error. For calculations, CHEMTAX program assumed that pigment:Chl_a ratios were constant within each phytoplankton pigment type in the entire set of samples. To satisfy this assumption, the final data set (n = 165) was divided so that environmental and therefore physiological conditions of phytoplankton were homogeneous within each subset. For this, a cluster analysis was carried out taking as classifying variables the Simpson's parameter, temperature and nitrate concentration as the limiting nutrient. Two groups were obtained: one corresponding to the warm-stratified period (n

= 26) and another to the cold-homogeneous period (n = 139). For each subset (winter-summer) an initial matrix of pigment:Chl_a relationships was generated and the program was executed.

Construction of PPT matrices and pigment relationships

The selection of PPTs included in the initial CHEMTAX matrices was based on pigments determined in samples, published microscopy information for the picoplankton fraction of the EPEA time series (Silva et al. 2009; Silva 2011) and several institutional campaign reports or unpublished data for other size fractions ('grey literature', not available to the international scientific community). The nomenclature proposed by Llewellyn et al. (2011) was used to name PPTs and pigments. Pigment:Chl_a ratios used in the initial CHEMTAX matrices were obtained from cultures of isolated species at the EPEA station (Montoya et al. 2015), pigments analysis of monospecific blooms samples from the area (Ruiz et al. 2023) and from the literature (Table 1).

Initial ratio values were identical for winter and summer matrices, except for the PPT CYANO-2 (cyanobacteria with Zea, example: genus *Synnechococcus* sp.), which is known to show higher Zea:Chl_a ratio values in summer.

Three groups of haptophytes were considered for the summer matrix: HAPTO-6 (e.g. *E. huxleyi*), HAPTO-7 (e.g. *Crysochromulina* sp.) and a group defined as 'HAPTO-P' to separate the contribution of a particular bloom of *Primnesium* sp. with high concentrations of MVChl_c3 (Negri 2005; Ruiz et al. 2023; see Discussion section). The MVChl_c3 differs from Chl_c3 in that it has a single vinyl group, which gives it slightly more polarity and an additional absorption peak at 630 nm. These characteristics result in a shorter retention time and a different absorption spectrum, allowing these pigments to be separated using the chromatographic method of Zapata et al. (2000). Thus, MVChl_c3 as marker pigment of HAPTO-P was only included in the summer matrix and, in contrast, only one group of haptophytes was included in the winter matrix, HAPTO-6. Also, PPTs PRASINO-3 (Prasinophyceae with Chl_b and Pras, e.g. *Pycnococcus provasolii*), CRYPTO-1 (Cryptophycea with Allo e.g.: genus *Hemiselmis* sp. and *Plagioselmis* sp.) and PELAGO-1 (algae with the carotenoid But_fuco, which includes silicoflagellates, dictiocae and pelagophytes) were included in both matrices. Two PPTs dinoflagellates containing DINO-1 (dinoflagellates with Peri, e.g. *A. tamarense*/*catenella* complex and *G. catenatum*, among others) and DINO-4 (dinoflagellates with Allo e.g. *Dinophysis acuminata*, *D. caudata* and *D. tripos*) were considered, the latest only for the summer matrix. Regarding the great variety of diatom species reported, DIATO-1 (e.g. *Chaetoceros didymus*) and DIATO-2 (e.g. *Rhizosolenia setigera and Pseudo-nitzschia* sp.) PPTs were included, but DIATO-2 only in winter.

Analysis of phytoplankton size structure based on DPs

To estimate phytoplankton size fractions, we compared equations of Uitz et al. (2006) with those proposed by Chase et al. (2020). This model is distinguished from that of Uitz in that it assigns half of the Chl_b concentration to picoplankton and the other half to nanoplankton, half of the Fuco concentration to microplankton and the other half to nanoplankton, 75% of the Peri concentration al nanoplankton and only 25% to microplankton (Table 2).

RESULTS

Annual cycle of environmental properties

Water column temperature oscillated between 8 °C and 23 °C, with minimum temperatures occurring in late July, August and September, and

Table 1. Initial pigment ratios used in the CHEMTAX analysis. The PPTs from diatoms, dinoflagellates and haptophytes differed between winter and summer subsets based on their respective observed frequencies. Initial pigment:Chl_a ratios were the same in both matrices except for Zea in CYANO-2.

Summer	Chl_c3	MV Chl_c3	Chl_c1	Peri	But_fuco	Fuco	Neo	Pras	Viola	Hex_fuco	Allo	Zea	Chl_b	Chl_c2_ MGD [18:4/14:0]	Chl_a
CYANO-2	0	0	0	0	0	0	0	0	0	0	0	1,530	0	0	1
PRASINO-3	0	0	0	0	0	0	0,098	0,085	0,082	0	0	0,033	0,975	0	1
CRYPTO-1	0	0	0	0	0	0	0	0	0	0	0,270	0	0	0	1
DINO-4	0	0	0	0	0	0	0	0	0	0	0,163	0	0	0	1
HAPTO-P	0,018	0,123	0,033	0	0	0,861	0	0	0	0	0	0	0	0	1
HAPTO-6	0,140	0	0	0	0,238	0,282	0	0	0	0,619	0	0	0	0,047	1
HAPTO-7	0,605	0	0	0	0	0,387	0	0	0	0,472	0	0	0	0	1
PELAGO-1	0,125	0	0	0	0,542	0,228	0	0	0	0	0	0	0	0	1
DINO-1	0	0	0	0,955	0	0	0	0	0	0	0	0	0	0	1
DIATO-1	0	0	0,055	0	0	0,654	0	0	0	0	0	0	0	0	1

Winter	Chl_c3	Chl_c1	Peri	But_fuco	Fuco	Neo	Pras	Viola	Hex_fuco	Allo	Zea	Chl_b	Chl_c2_ MGD [18:4/14:0]	Chl_a
CYANO-2	0	0	0	0	0	0	0	0	0	0	0,656	0	0	1
PRASINO-3	0	0	0	0	0	0,099	0,398	0,040	0	0	0,030	0,790	0	1
CRYPTO-1	0	0	0	0	0	0	0	0	0	0,350	0	0	0	1
HAPTO-6	0,140	0	0	0,238	0,282	0	0	0	0,619	0	0	0	0,047	1
PELAGO-1	0,121	0	0	0,607	0,264	0	0	0	0	0	0	0	0	1
DINO-1	0	0	0,955	0	0	0	0	0	0	0	0	0	0	1
DIATO-1	0	0,055	0	0	0,654	0	0	0	0	0	0	0	0	1
DIATO-2	0,065	0	0	0	1,099	0	0	0	0	0	0	0	0	1

Table 2. Formula used to calculate phytoplankton size fractions micro (F_{micro}), nano (F_{nano}) and picoplankton (F_{pico}) based on two different pigment indexes. DPw = weighted sum of diagnostic pigments concentration (mgm^{-3}); DP$w = \Sigma^{7}_{i=1}\, w_i\, P_i$, where w = weighted weight (dimensionless) and P = pigment concentration (mgm^{-3}).

Pigment (P_i)	Uitz indexes (w_i)	Uitz equations	Chase equations
Fuco (P_1)	1,41		
Peri (P_2)	1,41	$F_{micro} = \frac{\sum_{i=1}^{2} w_i P_i}{DP_w}$	$F_{micro} = \frac{0{,}5\ .\ w_1P_1 + 0{,}25\ .\ w_2P_2}{DP_w}$
Hex_fuco (P_3)	1,27		
But_fuco (P_4)	0,35	$F_{nano} = \frac{\sum_{i=3}^{5} w_i P_i}{DP_w}$	$F_{nano} = \frac{0{,}5\ w_iP_1 + 0{,}75\, w_2P_2 + \sum_{i=3}^{5} w_iP_i + 0{,}5\, w_6P_6}{DP_w}$
Allo (P_5)	0,60		
Chl_b (P_6)	1,01	$F_{pico} = \frac{\sum_{i=6}^{7} w_i P_i}{DP_w}$	$F_{pico} = \frac{0{,}5\ .\ w_6P_6 + w_7P_7}{DP_w}$
Zea (P_7)	0,86		

maximum between January and early March, with greater seasonal amplitude on the surface than at the bottom (Figure 2). The water column was homogeneous during the cold period (June-September, φ < Q1), and slowly stratified from the beginning of spring in October until reaching the maximum values of the Simpson parameter in summer, between January and March (φ > Q3) (Figure 2). Typically, salinity ranged between 33.3-33.7, although low salinity values < 33.5 were registered sporadically (April-May 1998: minimum 27.25) and high values (salinity > 33.90) were observed along the entire annual cycle. No seasonality was observed for low salinity values, while for high salinity values the highest occurrence was observed during autumn-early winter months (Figure 3).

Nitrate concentration ranged mainly between 0.010 and 5.000 μM, although values > 5.000 μM were observed particularly at greater depths during the summer (December-January). Similarly, silicate also showed higher values at greater depths, ranging between 0.016 and 10.670 μM. Regarding the nitrite ion, concentration values were lower than those of nitrate, as expected, and ranged between 0.010 and 1.910 μM. On the contrary, phosphate did not show a large variation with depth and its values ranged between 0.120 and 2.180 μM. The concentration of nitrates showed a marked cyclical seasonal variation with maximum concentrations during the winter (July-August), as did that of phosphate, although this was less pronounced (Figure 4). The concentration of other macronutrients studied did not show a particular mode of evolution throughout the year, presenting variable concentrations within defined limits. It should be noted that the highest nitrate concentration values corresponded to samples obtained from greater depths during December and January, which were associated with lowest temperatures recorded throughout the entire time series. In these stations, but at lower depths, the concentration of nitrates was lower with values similar to the rest of the time series and associated with higher temperatures, which demonstrates the early establishment of the thermocline in summer (Figure 4).

Phytoplankton pigment diversity

A total of 34 pigments were identified at the EPEA station, some of them in most of the samples and others rarely or in very low concentration (Table 3). The maximum Chl_a concentration

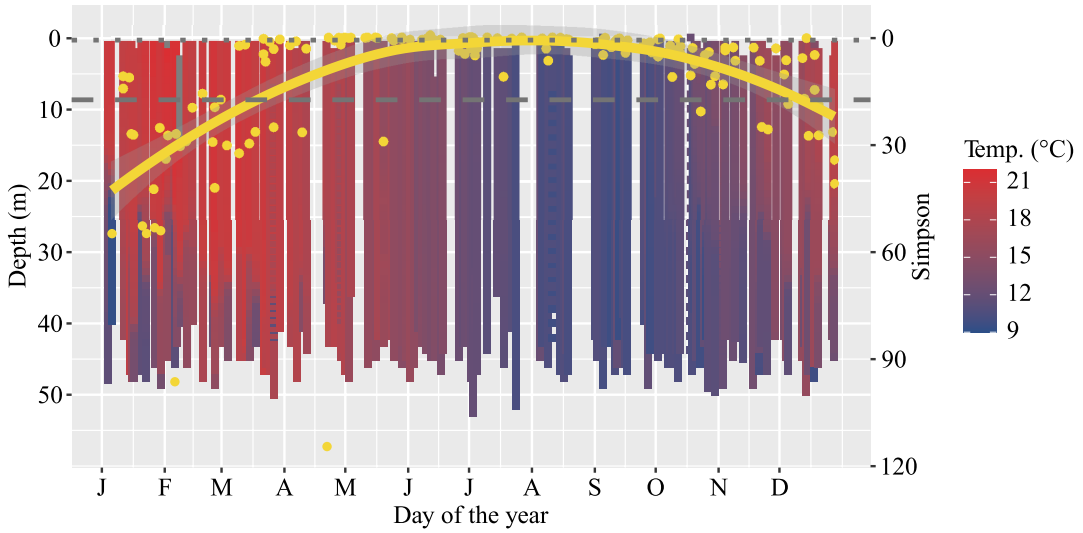

Figure 2. Water temperature as a function of depth and day of the year at EPEA station time series based on CTD data (period 1994-2019, n = 190 CTD profiles). In yellow, the Simpson parameter values (points), and superimposed on them, a local weighted regression (yellow line). Dotted and dashed grey horizontal lines indicate Simpson's quartiles Q1 and Q3, respectively (Q1 = 1.028 Jm^{-3} and Q3 = 34.529 Jm^{-3}). Letters on the horizontal axis indicate the beginning of the corresponding month. Temperature scale is shown in the right color bar, with reddish indicating warmer and blueish colder values.

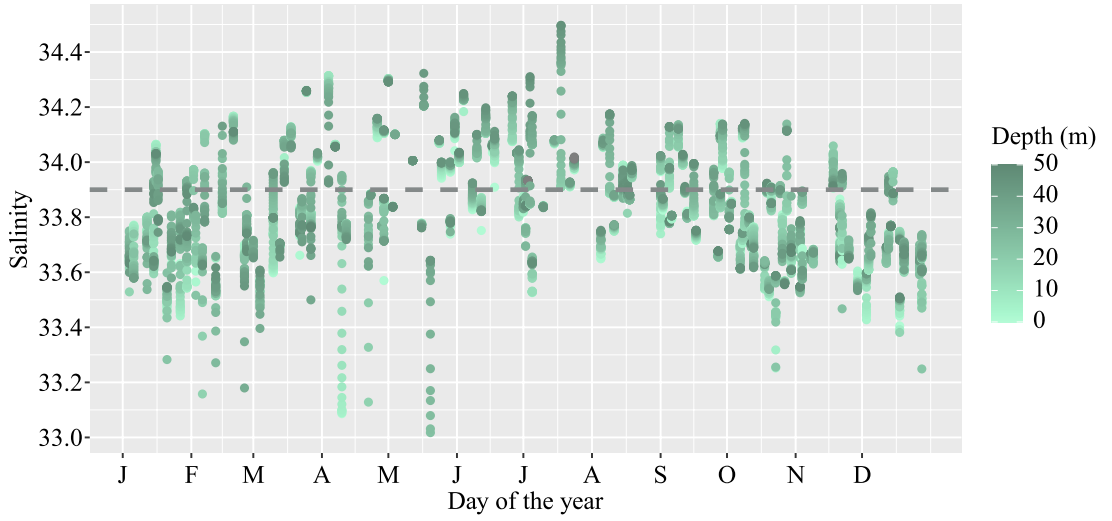

Figure 3. Salinity as a function of day of the year at EPEA station time series based on CTD data (period 1994-2019, n = 190 CTD profiles). Depth (m) is expressed in the *z* dimension (right color bar; maximum depth at EPEA = 48 m). Letters on the horizontal axis indicate the beginning of the corresponding month.

value determined by HPLC (8.301 mgm^{-3}) was associated with the maximum concentration of Fuco (5.404 mgm^{-3}; the main diatom marker) and also with the maximum of Allo (marker pigment for cryptophytes and dinoflagellates of the DINO-4 PPT) during April 2019, in what appeared to be a bloom dominated by more than one phytoplankton group. In contrast, the second highest

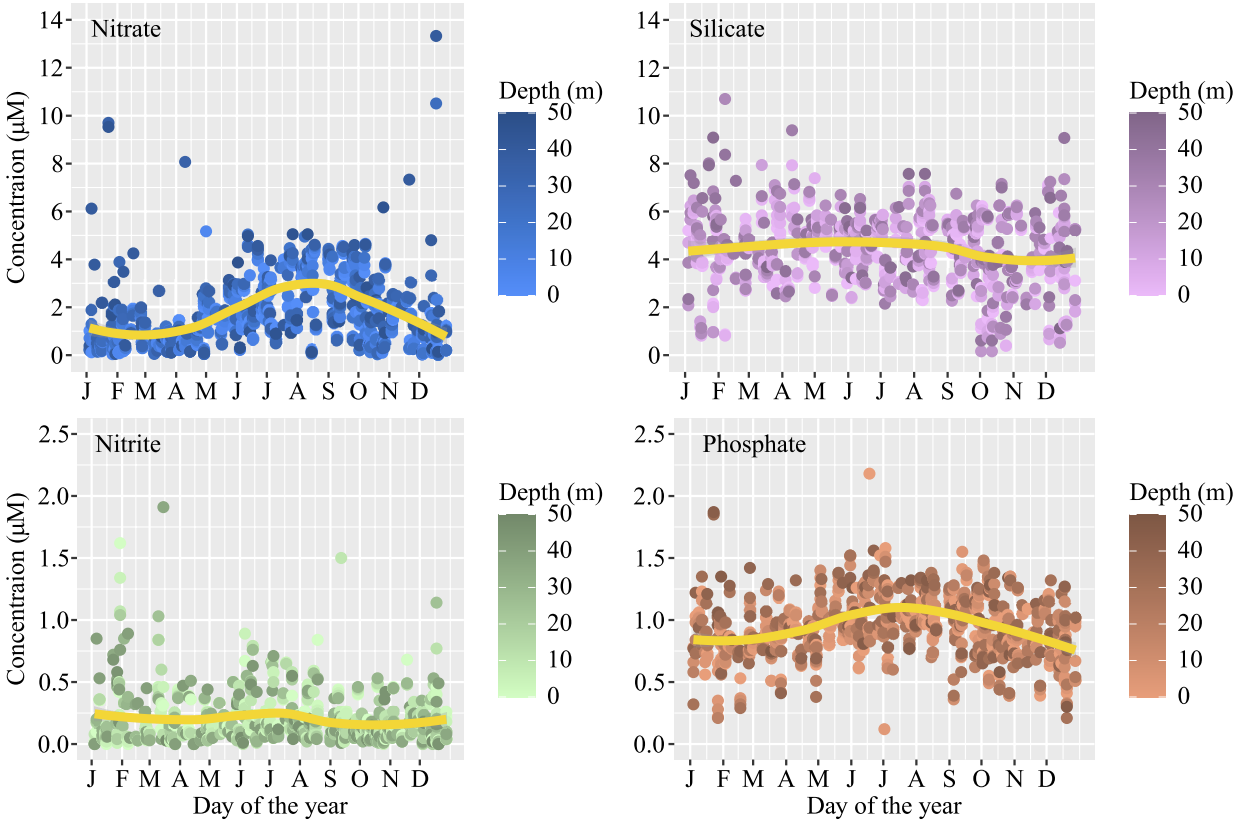

Figure 4. Concentration of main macronutrients determined at EPEA station in the period 1994-2019 (n = 934). Sampling depth (m) is expressed in the *z* dimension (right color bar; maximum depth at EPEA = 48 m). Orange line corresponds to a local weighted regression. Letters on the horizontal axis indicate the beginning of the corresponding month.

recorded concentration of Fuco (4.498 mgm^{-3}) occurred in a late spring bloom in November 2005, associated with high concentrations of MVChl_c3 (0.510 mgm^{-3}) and low concentrations of Hex_fuco (0.060 mgm^{-3}). Regarding Peri, the unequivocal marker pigment for dinoflagellates of the DINO-1 PPT, the maximum recorded concentration (3.236 mgm^{-3}) occurred in October 2019 and it was followed in magnitude by the record of April 2019 (0.563 mgm^{-3}). Chl_b, present in green algae, and Pras, present in prasinophytes, were found at very high frequency (Table 3). Although pigment sampling at this study site was stopped between 2005 and 2012, these values were representative of the relative magnitude of bloom events at this coastal location. The Chl_a annual cycle showed higher concentration values in winter (Figure 5), and Fuco presented the same seasonal pattern. On the other hand, Peri concentration followed a bimodal cycle, increasing notably in autumn and spring. Hex_fuco, marker pigment for haptophytes, also showed a bimodal pattern, although its concentration was on average 50% lower than that of Peri. For its part, both Zea (marker pigment for cyanobacteria) and But_fuco increased their concentration during summer months (December, January and February), when the water column begins to get stratified. It should be noted that, except for special events, the Chl_a concentration range throughout the year was small and, therefore, that of the other pigments even smaller.

Table 3. Average concentration (mgm^{-3}) and frequency (N) of phytoplankton pigments detected in the study site in the period 2000-2005 and 2012-2019. Conventional name and international abbreviation used in this work were indicated. Pigments were arranged in descending order of frequency of appearance at the study site.

Pigment	Abbreviation	Mean concentration	Standard deviation	Minimun	Maximun	N
Chlorophyll *a*	Chl_a	1.012	0.916	0.157	**8.301**	171
Fucoxanthin	Fuco	0.430	0.632	0.038	**5.404**	170
Chlorophyll *c*2	Chl_c2	0.152	0.206	0.009	1.732	167
19'-hexanoyloxyfucoxanthin	Hex_fuco	0.07	0.049	0.004	0.294	161
Diadinoxanthin	Diadino	0.087	0.136	0.007	1.553	160
Chlorophyll *b*	Chl_b	0.080	0.052	0.004	0.297	159
Chlorophyll *c*3	Chl_c3	0.044	0.047	0.003	0.367	159
Peridinin	Peri	0.108	0.275	0.006	**3.236**	149
Alloxanthin	Allo	0.038	0.070	0.001	**0.782**	137
19'-butanoyloxyfucoxanthin	But_fuco	0.027	0.033	0.001	0.247	132
Magnesium divinylpheoporphyrin	MgDVP	0.015	0.022	0.002	0.230	128
Prasinoxanthin	Pras	0.021	0.017	0.002	0.118	124
Neoxanthin	Neo	0.015	0.009	0.002	0.049	120
Chlorophyll *c*1	Chl_c1	0.031	0.042	0.001	0.283	119
ββ-carotene	b_Car	0.025	0.039	0.002	0.301	114
Zeaxanthin	Zea	0.028	0.070	0.001	**0.720**	112
Violaxanthin	Viola	0.015	0.009	0.001	0.049	108
4-keto-19'-hexanoyloxyfucoxanthin	Hex_kfuco	0.016	0.012	0.001	0.055	98
Non-polar chlorophyll of *Emiliania huxleyi*	Chl_c2_MGDG [18:4/14:0]	0.013	0.024	0.001	0.200	92
Chlorophyll *a* allomer	Chla_allomer	0.066	0.153	0.001	1.020	90
βε carotene	a_Car	0.010	0.008	0.001	0.035	79
Diatoxanthin	Diato	0.026	0.078	0.001	0.653	76
Chlorophyll *a* epimer	Chla_epimer	0.020	0.022	0.003	0.137	59
Lutein	Lut	0.010	0.008	0.001	0.041	57
Non-polar chlorophyll of *Chrysocromulina* sp.	Chl_c2_MGDG [14:0/14:0]	0.007	0.014	0.001	0.071	48
Chlorophyllide *a*	Chlide	0.061	0.254	0.001	1.622	40
Dinoxanthin	Dino	0.014	0.021	0.002	0.128	40
Antheraxanthin	Anth	0.034	0.093	0.002	0.480	26
Monovinyl chlorophyll *c*3	MVChl_c3	0.047	0.110	0.001	0.510	26
Methylchlorophyllide *a*	MeChlide	0.073	0.144	0.002	0.479	10
Pheophytin	Phe	0.136	0.173	0.011	0.463	6
Peridididinol	peridididinol	0.025	0.010	0.011	0.033	4
DehydroLutein	dehidroLuteina	0.012	0.004	0.008	0.015	3
Uriolide	Uri	0.015	0.006	0.009	0.021	3

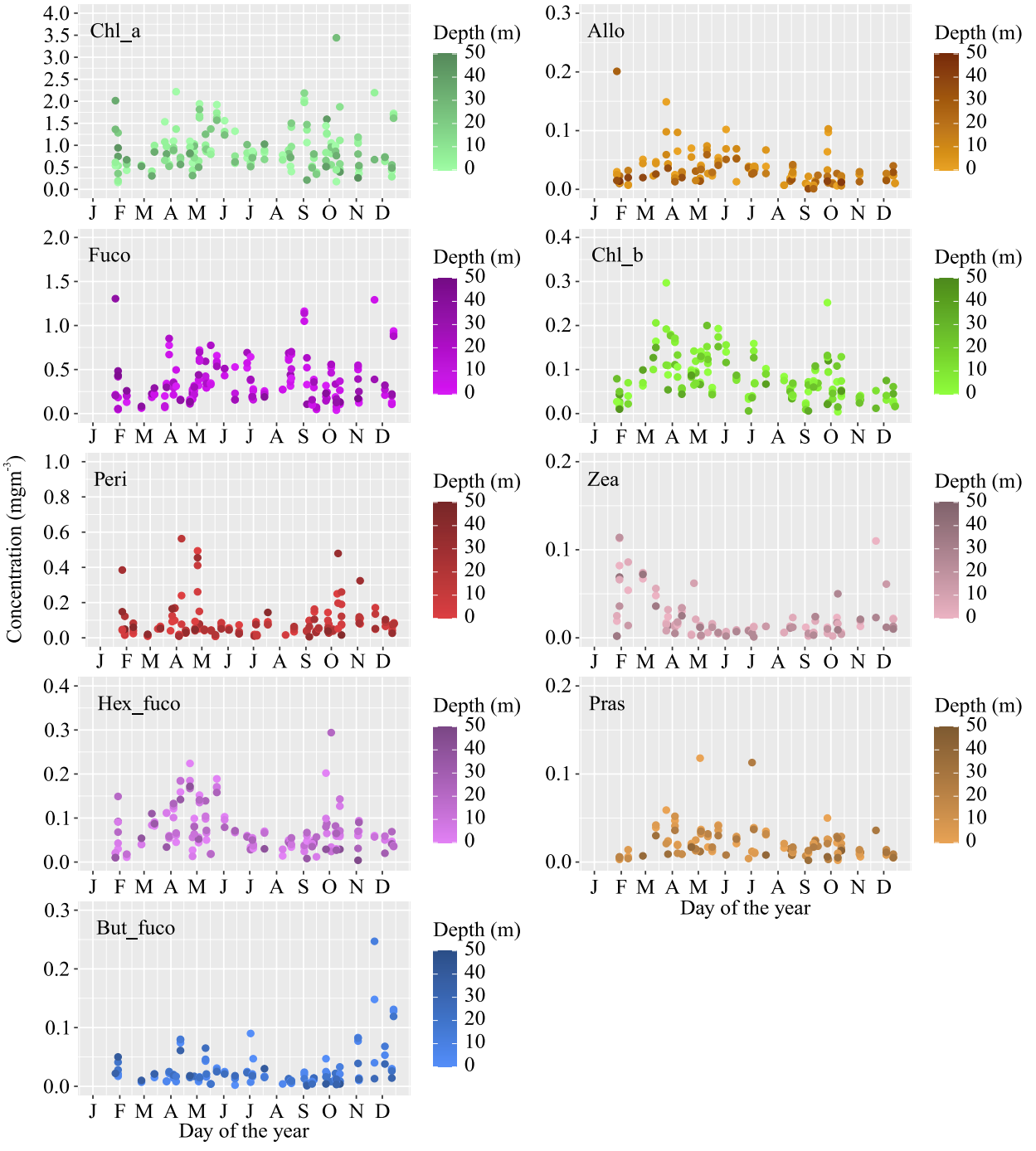

Figure 5. Annual cycle of main phytoplankton pigments concentration found at EPEA station. Note differences in the concentration scale of each pigment. Maximum values corresponding to infrequent bloom events were excluded for greater appreciation of the variability throughout the year (see Table 3). Letters on the horizontal axis indicate the beginning of the corresponding month.

Phytoplankton community size structure

The models of Uitz et al. (2006) and Chase et al. (2020) estimated different percentages of the phytoplankton size fractions (micro, nano and picoplankton) throughout the annual cycle based on the analysis of DPs (Figure 6). Uitz's model estimated that microplankton makes up on average 80% of the community throughout the year, with a slight decrease towards summer, while Chase's model estimated an average of 40% for this fraction. According to Chase, nanoplankton was the dominant fraction throughout the annual cycle (average 60%), which was more than double of that estimated by the Uitz model (20%). Both models agreed that picoplankton reached its maximum in January-February (making up to 40%) and hovers around 10-20% during the rest of the year.

Annual cycle of Phytoplankton Pigmentary Types estimated by CHEMTAX

Only two CHEMTAX cycles were enough to optimize the pigment:Chl_a ratios in each matrix until reaching acceptable residual levels of pigments according to the standards established in the method (Mackey et al. 1996). The Chl_a concentration contributed by each PPT in each sample was then estimated by CHEMTAX and the relative contribution of each PPT over the annual cycle was calculated (Figure 7). During winter months (June-August), biomass was dominated by diatoms, contributing more than 50% of Chl_a, with the greatest contribution from PPT DIATO-2, i.e. diatoms containing Chl_c3. DIATO-2 abundance was relatively higher at greater depths than DIATO-1. As spring progresses, diatoms decline and dinoflagellates with peridinin, the PPT DINO-1, increases their representation, even reaching levels of up to 90% of total Chl_a. Altogether, different types of haptophytes (HAPTO-6, HAPTO-7 and HAPTO-P) also thrived at this time of year, sustaining levels close to 20% of the total Chl_a throughout the summer. In the summer period, other groups such as CYANO-2, formed by cyanobacteria of the type *Synechococcus* sp. increased their biomass, especially in December-January, although their contribution occasionally exceeds 10% of the total Chl_a, and

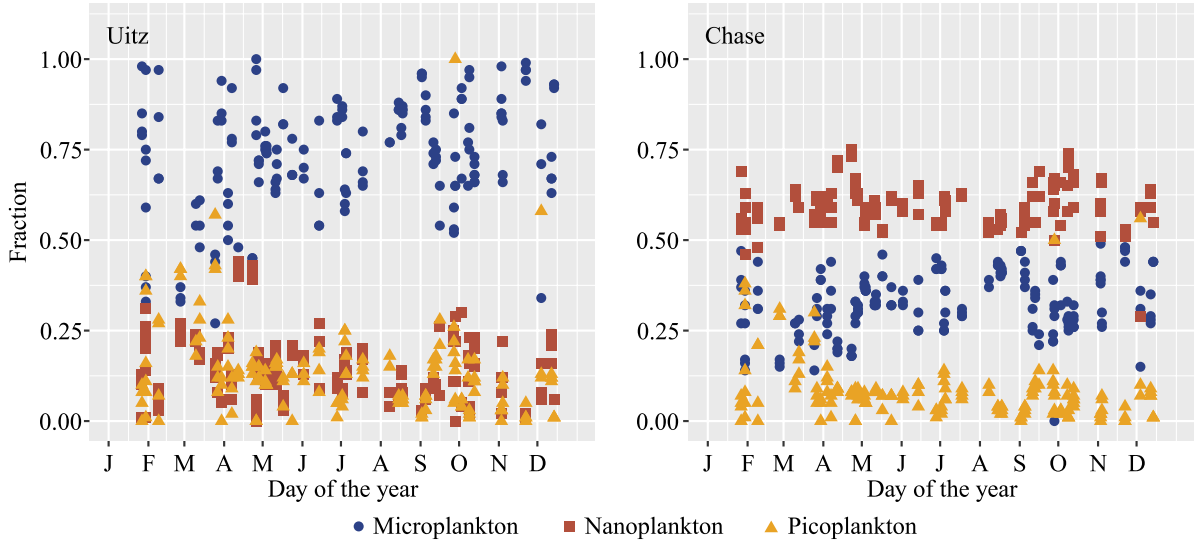

Figure 6. Annual cycle of phytoplankton size fractions estimated indirectly from pigment indices and the equations proposed by Uitz et al. (2006) and Chase et al. (2020). Each fraction is expressed as a contributed percentage of total Chl_a concentration in each sample. Letters on the horizontal axis indicate the beginning of the corresponding month.

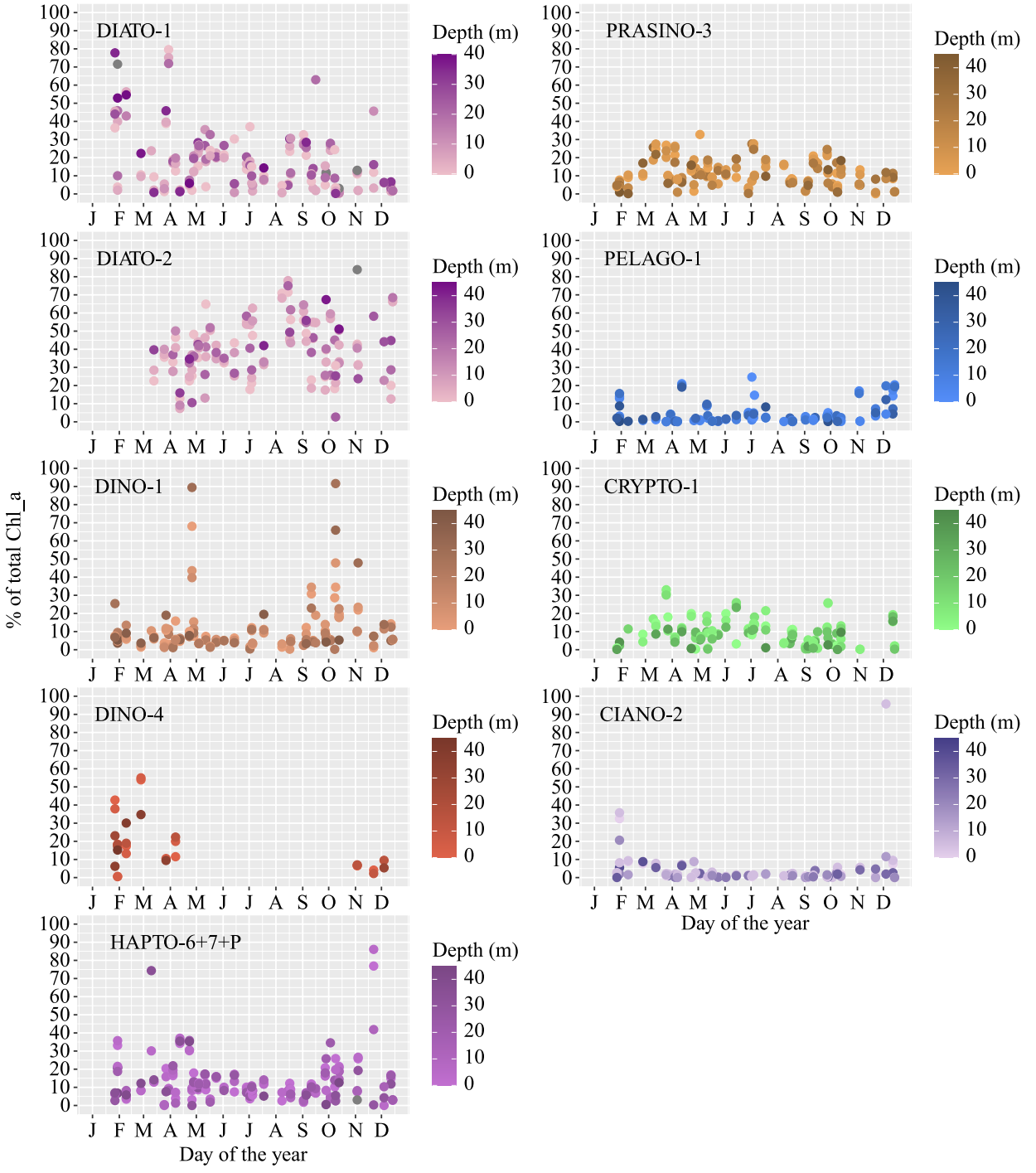

Figure 7. Annual cycle of different phytoplankton groups defined as phytoplankton pigmentary types (PPTs) expressed as relative contribution to the total Chl_a concentration in each sample. Letters on the horizontal axis indicate the beginning of the corresponding month.

dinoflagellates with Allo, such as DINO-4, can represent up to 40% of the total Chl_a. Other groups such as PRASINO-3, CRYPTO-1 and PELAGO-1 were present throughout the year, contributing on average 25% of the total biomass.

The CHEMTAX analysis revealed the relative abundance of three PPTs to which potentially toxin-producing phytoplankton species belong, which were maximum under different hydrological conditions (Figure 8). The PPT DINO-1 (represented by the paralyzing shellfish toxin producers *G. catenatum* and *A. tamarense*/*catenella* complex), presented an autumn bloom during April when the concentration of nitrate begins to increase after summer consumption, which is characterized by temperatures close to 18 °C, salinity in the range of 34.0-34.2, and weak stratification conditions. In contrast, DINO-1 spring bloom takes place during October at lower temperatures of 10-12 °C and slightly lower salinity of 33.8-34.0, under conditions where the column begins to stratify and nitrate concentration is not limiting. On the contrary, the abundance of PPT DINO-4, group housing the genus *Dinophysis* sp. to which several species producing lipophilic toxins belongs, was highest during the summer months of January and February when temperature exceeded 18 °C, salinity was > 33.7 and the water column presented maximum stratification. Finally, DIATO-2 (PPT containing potentially DA producer species such as *Pseudo-nitzschia* sp.), had maximum abundances at the end of winter (August and September) under conditions where the column was completely mixed, nitrate concentration was high, average temperature was 10 °C and salinity was between 33.8-34.0.

DISCUSSION

The composition and size structure of the phytoplankton community has been characterized through the chemotaxonomic approach in a coastal site throughout the annual cycle in relation to environmental conditions.

Located at 27 nmi from Mar del Plata city, the study site has a marked seasonal pattern of thermocline formation and rupture, with incident irradiance being one of its main drivers (Carreto et al. 2004; Lutz et al. 2006; Viñas et al. 2013; Ruiz 2018; Ruiz et al. 2020). Stratification breakdown occurs more slowly than the thermocline establishment. The EPEA station is bathed by a single water mass, the Subantarctic Shelf Waters (ASAP), which is

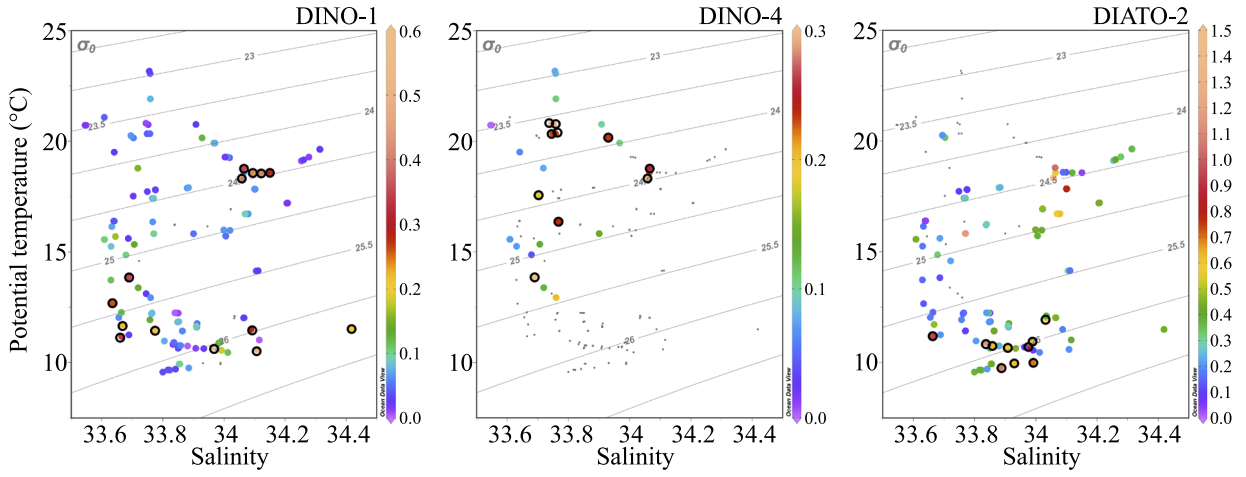

Figure 8. Relative abundance of PPTs having toxin-producing species recorded at the EPEA station during the study period, expressed as the contribution to the total concentration of Chl_a (mgm^{-3}) in the temperature-salinity diagrams.

modified as it travels along the continental shelf (Guerrero and Piola 1997). At the study site, salinity values > 33.9 were observed during fall-early winter, denoting the influence of high salinity coastal waters originating in the summer in the San Matías Gulf due to excess evaporation over precipitation and advected to these latitudes. Further, the influence of low-salinity diluted waters was observed in different years, driving salinity values at this latitude to < 33.4, even at depth. Apart from these two phenomena, no other phenomenon establishing seasonality in salinity was observed at the EPEA station. Nutrient enrichment is provided by ASAP, as well as vertical mixing taking place mainly during July-September. Therefore, nitrate concentration follows this cycle with higher values during winter and lower in summer, mainly due to spring consumption of phytoplankton. Silicate and phosphate concentrations vary little throughout the year and do not appear to limit phytoplankton growth.

It has been shown that the period between June and October coincides with the lowest Simpson parameter values, coldest temperatures and higher nitrate concentrations. Also, the depth of the euphotic zone is minimum during these months at this study site (Lutz et al. 2006; Ruiz 2018; Ruiz et al. 2020). These conditions seem to support the development of diatoms groups (DIATO-1 and DIATO-2), which dominated phytoplankton biomass in terms of Chl_a concentration contribution. The predominance of diatoms is typical of temperate seas, similar to what was previously described for this site (Carreto et al. 2004; Negri and Silva 2011). Despite the relatively low light availability, diatom growth could be favored by strong vertical mixing driving cells towards the illuminated layer with a frequency high enough to allow growth. The total biomass of phytoplankton decreases in October as the thermocline is established and nutrient consumption progresses. In turn, the relative contribution of various PPTs increases, resulting in a more diverse community. On average, the contribution of DIATO-1 and DIATO-2 to phytoplankton biomass start to decrease, while that of other groups becomes more conspicuous, mainly DINO-1, DINO-4 and haptophyte groups. It is known that under conditions of high irradiance and low nutrient availability, smaller cells outperform larger ones by having a higher surface/volume ratio, giving them greater efficiency in nutrient uptake. Consequently, a change in community size structure toward summer can be suspected.

Two pigment-based size indices have been used to examine the size structure of the phytoplankton community. The main difference between the two is that the Chase index considers the contribution of diatoms and dinoflagellates to the nanoplankton fraction (Chase et al. 2020). According to differences in their equations, these indices showed different results regarding micro- and nanoplankton fractions, but, contrary to expectations, none showed seasonal variability. However, it can be assumed that the phytoplankton community presents a change in size structure considering the observed increase in the concentration of typical pigments of nanoplankton species (Hex_fuco, Zea, Chl_b, But_fuco, peri and Fuco) during the stratified period. This, in turn, was reflected in the relatively higher abundance during this period of the haptophyte PPTs, PELAGO-1, CYANO-2, DINO-1, and CRYPTO-1. Likewise, previous studies demonstrated that some bio-optical parameters associated with small cells also showed relative increases during the stratified period at the study site (Ruiz et al. 2020). The relative abundance of PPTs to which cyanobacteria and cryptophytes belong was higher in summer, as previously observed at the EPEA station (Silva et al. 2009; Silva 2011). The HAPTO-6, HAPTO-7 and HAPTO-8 and PELAGO-1 groups, among others, made a greater contribution to the phytoplankton biomass during the stratified period. When considering that the average 60 % estimated by the model of Chase et al (2020) for the nanoplankton fraction is composed primarily of diatoms, dinoflagellates, haptophytes, and pelagophytes, it appears to be more approximate than that of Uitz et al. (2006) to estimate the size fractions using DPs. This is because haptophytes correspond to the nano

and picoplankton fraction. However, these models will need to be validated with direct estimates of cell size obtained through microscopy or new optical analysis techniques such as flow imaging.

Some blooms events were registered at the EPEA station during the study. A multispecies algal bloom occurred in autumn 2019, with diatoms (DIATO-2 and DIATO-1) accounting for nearly 70% of the Chl_a produced, followed by DINO-4 which contributed 22% of Chl_a and DINO-1 with 5%. Fuco was mainly contributed by diatoms of the genus *Chaetocelos* sp., including *C. curvisetus*, *C. decipiens* and *C. danicus*, while Allo was due to *D. tripos*, a species that produced PTX2 and sec PTX2 (Negri 2019). Regarding DINO-1 dinoflagellates, the spring bloom in October 2019 was dominated by an unarmored dinoflagellate of the genus *Gymnodinium* sp. (Ruiz et al. 2023), and the autumn bloom of 2000 was dominated by the *A. tamaense/catenella* complex with paralyzing toxin detected in mussels collected at the site (Carreto et al. 2004). Only once an extraordinary growth of *Synechococcus* sp. was observed in early summer (Ruiz et al. 2020), which explains the high levels of Zea concentration registered at the surface layer. Regarding the late spring bloom in November 2005, associated with high MVChl_c3 and low Hex_fuco concentrations, Negri (2005) reported the dominance of an indeterminate species of *Prymnesium* sp. (Prymnesiophyceae), a haptophyte that caused a bright green surface discoloration with concentrations of at least 12 x 10^6 cells l^{-1} and characterized by a '… total absence of diatoms…' (Negri 2005). Zapata et al. (2004) described eight different haptophyte PPTs based on their pigment suits and pigment:Chl_a ratios. According to this study, Prymnesiophyceae belongs to HAPTO-4 (lacking Hex-fuco and MVChl_c3) and *E. huxleyi*-type coccolithophorids belong to HAPTO-6 (with MVChl_c3 and Hex-fuco, among other pigments). In this event, a high concentration of MVChl_c3 was determined, which is a characteristic pigment of HAPTO-6 but absent in HAPTO-4. For this reason, the PPT 'HAPTO-P' was defined to resolve the contribution to the total Chl_a concentration of samples from this event. Evidently, this is a type of prymnesiophyte having MVChl_c3, since in the presence of HAPTO-6 in the sample was ruled out based on the taxonomic determination (Negri 2005) and also due to the Hex_fuco:Chl_a ratio observed, which was much lower than expected for the group (0.010 < 0.629). To our knowledge, this is the first record of a primnesiophyte possessing MVChl_c3.

The annual cycle of two different groups of dinoflagellates at EPEA station was revealed by the CHEMTAX. On the one hand, PPT DINO-1, which groups species with carotenoid Peri as an unequivocal marker, and on the other, DINO-4, a group including dinoflagellates with Allo. Both PPTs host, on the one hand, the main harmful species described for the coast of Buenos Aires province, *A. tamarense*/*catenella* complex and *G. catenatum*, producers of PSP, and on the other, the genus *Dinophysis* sp., producer of lipophilic toxins, respectively. Dinoflagellates contribution to total Chl_a was considerably lower than that of diatoms, partly due to their lower abundance and also to the presence of smaller cell-sized nanoplanktonic dinoflagellates (Silva, personal communication).

As in previous works (Carreto et al. 2004), a bimodal cycle was revealed for the PPT DINO-1, an autumn bloom just before the beginning of the of greatest vertical mixing period, and another in spring coinciding with the beginning of the heating and stratification of the water column. Environmental conditions are very different at these two moments of the annual cycle. The autumn bloom at the EPEA station may be dominated by *G. catenatum*, whereas in the spring bloom *A. tamarense*/*catenella* complex (Méndez and Carreto 2018) dominates, although this should be fully confirmed by more in-depth taxonomy studies across the entire time series. Previously, between 1994 and 1997, Akselman et al. (1998) associated the autumn PSP toxicity peak in *M. edulis* mussels with *G. catenatum* at a fixed station off Mar del Plata, also observing the absence of *A. tamarense*/*catenella* complex for this time of the year. Méndez

and Carreto (2018) described the ecology of these two species for the Río de la Plata front. Long-term studies have recorded several *G. catenatum* blooms on the Uruguayan coast with temperatures between 21.8 °C and 24.0 °C in late summer-autumn. These blooms eventually spread to higher latitudes along the Argentine coast. That is, *G. catenatum* often blooms at lower latitudes than the EPEA associated with relatively warm temperatures. Meanwhile, the growth of *A. tamarense*/*catenella* complex may be favored by periods of calm winds and high solar irradiation, such as those prevailing in spring at the study site (Carreto et al. 1993). The germination of resting cysts results in the first planktonic forms of *A. tamarense*/*catenella* complex in this region at the end of winter. This process is controlled by endogenous biological mechanisms synchronized by certain environmental factors, resulting in high interannual variability. However, several other dinoflagellate species with Peri are known (i.e. belonging PPT DINO-1), such as *Azadinium* sp., a genus capable of synthesizing azaspiracid phycotoxins (AZAs). *Azadinium* sp. was recorded in a broad range of environmental conditions along the southwestern Atlantic, including this study site (Akselman and Negri 2012; Akselman et al. 2014). Also, an extraordinary bloom of an unarmored *Gymnodinium* sp. was registered in October 2021 in the Argentine continental shelf, with Peri concentration of up to 69.197 mgm^{-3} on the surface (unpublished data).

Furthermore, the CHEMTAX effectively estimated the relative abundance of PPT DINO-4 (dinoflagellates with Allo). Interestingly, the highest abundance of DINO-4 was recorded throughout 2019. Negri (2019) reported the presence of *D. tripos* in summer close to the depth of the thermocline in the EPEA station. It has been documented that *Dinophysis* sp. growth is favored under conditions of high thermohaline stratification and persistent winds (Escalera et al. 2006, and references therein). On that occasion, cell abundance reached 36,700 cells l^{-1} and toxins pectenotoxin PTX2 and secacid PTX2 linked to the presence of *D. tripos* were recorded, while dinophysis toxins were not detected. It should be noted that PTXs have been removed from health standards for live bivalve mollusks since 2021 in accordance with current legislation, as the European Food Safety Authority (EFSA) recently concluded that there are no reports of adverse effects associated with PTXs in humans.

Theory behind CHEMTAX has been described extensively (Mackey et al. 1996). CHEMTAX main limitation lies in the fact that it is very sensitive to the initial ratio matrix. Small differences in initial pigment:Chla ratio values are not sufficient to estimate with good approximation the abundance of PPTs sharing the same pigment arrangement, such as haptophytes and diatoms, or haptophytes and pelagophytes. However, CHEMTAX's performance improves by applying various strategies in its execution. On the one hand, the RSM decreases if unambiguous marker pigments are included in the matrix (for example, gyroxanthin diester to estimate *Karenia brevis*, or as described above, MVChl_c3 to separate HAPTO-P), as well as if the pigments present in all groups are excluded, such as Chl_c2. Another strategy is to separate the samples into different run cycles based on the presence/absence of certain marker pigments and assemble the ratio matrices accordingly (e.g. run samples lacking Chl_c1 on a matrix that does not include DIATO-1). In this way, the probability that CHEMTAX assigns part of the total Chl_a to a PPT absent in the samples is reduced to zero. Finally, starting from the best possible approximation of pigment:Chl_a ratio values in each group improves the performance of the method. For example, pigment:Chl_a ratios in different haptophyte groups vary in very high ranges according to different physiological conditions (Schlüter et al. 2000; Zapata et al. 2004). In the present study, pigment:Chl_a ratios were determined from cultures or from *in situ* samples corresponding to blooms from the region (Ruiz et al. 2023), obtaining good results with CHEMTAX (low RMS in only two execution cycles). In summary, CHEMTAX should be regarded as a 'thick brush' tool for distribution

and biogeography studies that provides a very good approximation to the estimation of relative abundances, but not a way to discriminate down to the species level (except for a few particular cases).

Phytoplankton pigments constitute many more compounds than chlorophyll *a* that can be applied to study phytoplankton diversity or develop better primary production models. In recent years, several works have addressed the estimation of phytoplankton pigments from the remote sensing of ocean color. Without a doubt, the combination of the chemotaxonomic approach and the information from recently launched hyperspectral remote sensors will contribute to improve algorithm applicable to the study of the biogeography of different phytoplankton taxa, especially in sites where the early detection of potentially harmful blooms is desired. Although the toxicity of an event cannot be determined remotely, in the medium term the combination of these tools will be very useful to contribute to early warning systems of potentially harmful blooms for society and the ecosystem in general.

CONCLUSIONS

The present work is the first description of the composition of the phytoplankton community applying the chemotaxonomic approach (HPLC + CHEMTAX pigments) at the EPEA station, currently the longest time series of ecological observations in the southwestern Atlantic Ocean. Chemotaxonomy is shown to be a powerful tool for rapid and reproducible estimation of the relative abundance of different classes of phytoplankton in a large number of samples, including groups of interest for having toxin-producing species. Without a doubt, this tool will allow studying the ecology of harmful or toxic phytoplankton groups and making contributions to the knowledge of their seasonal or interannual variation in time series as well as in other coastal marine environments.

ACKNOWLEDGMENTS

INIDEP is the major financial source for the Estación Marea Roja/EPEA project. We are thankful for the collaboration of our past and current colleagues from different INIDEP Programs (QMAR, DIPLAMCC, GOF, Operations) that made the cruises and sampling possible. The help of the Captains and crews from INIDEP and Prefectura Naval Argentina vessels are very much appreciated. Special thanks to the anonymous reviewers who improved this manuscript. This is INIDEP contribution no 2367.

Author contributions

M. Guillermina Ruiz: conceptualization; software; formal analysis; investigation; data curation; writing-original and final draft; visualization. M. Belén Mattera Coy: data analysis; methodology. Mario C. Carignan: sampling; formal analysis; investigation; software; data curation. Macarena Albornoz: sample analysis; data curation; formal analysis. Graciela N. Molinari: software; validation; formal analysis; investigation; supervision. Nora G. Montoya: conceptualization; methodology; formal analysis; investigation; resources; writing-review and editing; supervision; project administration.

REFERENCES

Akselman R, Carreto JI, Montoya NG. 1998. *Gymnodinium catenatum* and autumn toxicity in northern shelf waters of Argentina. In: Reguera B, Blanco J, Fernández ML, Wyatt T, editors. Harmful Algae. Santiago de Compostela: Xunta de Galicia and Intergovernmental Oceanographic Commission of UNESCO. p. 122-123.

Akselman R, Negri RM. 2012. Blooms of *Aza-*

dinium cf. *spinosum* Elbrächter et Tillmann (Dinophyceae) in northern shelf waters of Argentina, Southwestern Atlantic. Harmful Algae. 19: 30-38.

Akselman R, Negri RM, Cozzolino E. 2014. *Azadinium* (Amphidomataceae, Dinophyceae) in the Southwest Atlantic: in situ and satellite observations. Rev Biol Mar Oceanog. 49: 511-526.

Armbrecht LH, Wright SW, Petocz P, Armand LK. 2015. A new approach to testing the agreement of two phytoplankton quantification techniques: microscopy and CHEMTAX. Limnol Oceanogr Methods. 13 (8): 425-437.

Armstrong FAJ, Stearns CR, Strickland JDH. 1967. The measurement of upwelling and subsequent biological process by means of the Technicon Autoanalyzer® and associated equipment. Deep-Sea Res. 14 (3): 381-389.

BaRDO. 2023. Base Regional de Datos Oceanográficos (BaRDO). Gabinete de Oceanografía Física. Mar del Plata: Instituto Nacional de Investigación y Desarrollo Pesquero (INIDEP). https://www.argentina.gob.ar/inidep.

Bouman H, Platt T, Sathyendranath S, Stuart V. 2005. Dependence of light-saturated photosynthesis on temperature and community structure. Deep-Sea Res I Oceanogr Res Pap. 52 (7): 1284-1299.

Brewin RJW, Sathyendranath S, Hirata T, Lavender SJ, Barciela RM, Hardman-Mountford NJ. 2010. A three-component model of phytoplankton size class for the Atlantic Ocean. Ecol Model. 221 (11): 1472-1483.

Cadaillón AM, Mattera B, Albizzi A, Montoya N, Maldonado S, Raya Rey A, Riccialdelli L, Almandoz GO, Schloss IR. 2024. Multispecies mass mortality in the Beagle Channel associated with paralytic shellfish toxins. Harmful Algae. 132: 102581.

Cai Y, Cao Y, Tang C. 2019. Evidence for the primary role of phytoplankton on nitrogen cycle in a subtropical reservoir: reflected by the stable isotope ratios of particulate nitrogen and total dissolved nitrogen. Front Microbiol. 10: 2202.

Carreto J, Montoya N, Akselman R, Negri R, Carignan M, Cucchi Colleoni A. 2004. Differences in the PSP toxin profiles of *Mytilus edulis* during spring and autumn blooms of *Alexandrium tamarense* off Mar del Plata coast, Argentina. In: Steidinger K, Landsberg J, Tomas C, Vargo G, editors. St. Petersburg Florida, USA. Florida Fish and Wildlife Conservation Commission, Florida Institute of Oceanography, and Intergovernmental Oceanographic Commission of UNESCO. p. 100-102.

Carreto J, Ramirez F, Roa B, Verona C. 1973. Plancton y condiciones ecológicas de la plataforma bonaerense, frente a Mar del Plata. II. Campaña "Transección II". FAO Documento Técnico Preliminar 30.

Carreto JI, Carignan MO, Montoya NG, Cozzolino E, Akselman R. 2018. Mycosporine-like amino acids and xanthophyll-cycle pigments favour a massive spring bloom development of the dinoflagellate Prorocentrum minimum in Grande Bay (Argentina), an ozone hole affected area. J Mar Syst. 178:15-28.

Carreto JI, Elbusto C, Sancho H, Carignan MO, Cucchi Colleoni AD, De Marco SG, Fernández A. 1993. An exploratory analysis of the Mar del Plata shellfish toxicity area (1980 1990). In: Smayda TJ, Shimizu Y, editors. Toxic phytoplankton blooms in the sea; Newport, Rhode Island, USA. Elsevier. p. 952.

Carreto JI, Montoya NG, Akselman R, Carignan MO, Silva RI, Colleoni DAC. 2008. Algal pigment patterns and phytoplankton assemblages in different water masses of the Río de la Plata maritime front. Cont Shelf Res. 28: 1589-1606.

Carreto JI, Montoya NG, Benavides HR, Guerrero R, Carignan MO. 2003. Characterization of spring phytoplankton communities in the Río de La Plata maritime front using pigment signatures and cell microscopy. Mar Biol. 143: 1013-1027.

Carreto JI, Montoya NG, Carignan MO, Akselman R, Acha EM, Derisio C. 2016. Envi-

ronmental and biological factors controlling the spring phytoplankton bloom at the Patagonian shelf-break front - Degraded fucoxanthin pigments and the importance of microzooplankton grazing. Prog Oceanogr. 146: 1-21.

Chase AP, Kramer SJ, Haëntjens N, Boss ES, Karp-Boss L, Edmondson M, Graff JR. 2020. Evaluation of diagnostic pigments to estimate phytoplankton size classes. Limnol Oceanogr Methods. 18 (10): 570-584.

Devred E, Sathyendranath S, Stuart V, Platt T. 2011. A three component classification of phytoplankton absorption spectra: application to ocean-color data. Remote Sens Environ. 115 (9): 2255-2266.

Escalera L, Reguera B, Pazos Y, Moroño A, Cabanas JM. 2006. Are different species of *Dinophysis* selected by climatological conditions? Afr J Mar Sci. 28 (2): 283-288.

[EURLMB] European Union Reference Laboratory for Marine Biotoxins. 2011. EU-Harmonised standard operating procedure for determination of lipophilic marine biotoxins in molluscs by LC-MS/MS. Vigo: EURLMB. https://www.aesan.gob.es/AECOSAN/docs/documentos/laboratorios/LNRBM/ARCHIVO2EU-Harmonised-SOP-LIPO-LCMSMS_Version5.pdf.

Fabro E, Almandoz GO, Ferrario M, John U, Tillmann U, Toebe K, Krock B, Cembella A. 2017. Morphological, molecular, and toxin analysis of field populations of *Alexandrium* genus from the Argentine Sea. J Phycol. 53 (6): 1206-1222.

Garrido JL, Zapata M. 1997. Reversed-phase high-performance liquid chromatographic separation of mono- and divinyl chlorophyll forms using pyridine-containing mobile phases and a polymeric octadecylsilica column. Chromatographia. 44 (1): 43-49.

Goela PC, Icely J, Cristina S, Danchenko S, Angel Delvalls T, Newton A. 2015. Using bio-optical parameters as a tool for detecting changes in the phytoplankton community (SW Portugal). Estuar Coast Shelf Sci. 167: 125-137.

Grasshoff K, Manfred E, Klaus K, editors. 1983. Methods of seawater analysis. 2nd ed. Weinheim: Verlag Chemie.

Guerrero R, Piola A. 1997. Masas de agua en la Plataforma Continental Argentina. In: Boschi EE, editor. El Mar Argentino y sus recursos pesqueros. Tomo 1. Antecedentes históricos de las exploraciones en el mar y las características ambientales. Mar del Plata: Instituto Nacional de Investigación y Desarrollo Pesquero (INIDEP). p. 107-118.

Hirata T, Aiken J, Hardman-Mountford, Smyth TJ, Barlow RG. 2008. An absorption model to determine phytoplankton size classes from satellite ocean colour. Remote Sens Environ. 112: 3153-3159.

Jeffrey SW, Mantoura RF, Wright SW. 1997. Phytoplankton pigments in oceanography: guidelines to modern methods. Paris: UNESCO. 661 p.

Jeffrey SW, Wright SW, Zapata M. 2011. Microalgal classes and their signature pigments. In: Roy S, Llewellyn CA, Egeland ES, Johnsen G, editors. Phytoplankton pigments: characterization, chemotaxonomy and applications in oceanography. Cambridge: Cambridge University Press. p. 3-77.

Krock B, Ferrario ME, Akselman R, Montoya NG. 2018. Occurrence of marine biotoxins and shellfish poisoning events and their causative organisms in Argentine marine waters. Oceanography. 31 (4): 132-144.

Lange KB. 1985. Spatial and seasonal variations of diatom assemblages off the Argentinean coast (South Western Atlantic). Oceanol Acta. 8 (3): 361-369.

Larios-Muñiz M, González-Silvera A, Castro R, Santamaría-Del-Ángel E, Collins CA, López-Calderón J. 2022. Variability of hydrographic factors, biomass and structure of the phytoplankton community at the entrance to the Gulf of California (spring 2013). Cont Shelf Res. 235: 104665.

Llewellyn CA, Egeland ES, Johnsen G, Roy S. 2011. Abbreviations and symbols. In: Roy S, Llewellyn CA, Egeland ES, Johnsen G, editors. Phytoplankton pigments: characterization, chemotaxonomy and applications in oceanography. Cambridge: Cambridge University Press. p. 25-28.

Lutz VA, Subramaniam A, Negri MR, Silva RI, Carreto JI. 2006. Annual variations in bio-optical properties at the "Estación Permanente de Estudios Ambientales (EPEA)" coastal station, Argentina. Cont Shelf Res. 26: 1093-1112.

Mackey MD, Mackey DJ, Higgins HW, Wright SW. 1996. Chemtax: a program for estimating class abundances from chemical markers: application to HPLC measurements of phytoplankton. Mar Ecol Prog Ser. 144 (1/3): 265-283.

Méndez SM, Carreto JI. 2018. Harmful Algal Blooms in the Río de la Plata Region. In: Hoffmeyer MS, Sabatini ME, Brandini FP, Calliari DL, Santinelli NH, editors. Plankton ecology of the Southwestern Atlantic: from the subtropical to the subantarctic realm. Cham: Springer International Publishing. p. 477-493.

Méndez SM, Medina D. 2004. Twenty-three years of red tide monitoring at fixed stations along the coast of Uruguay. In: Steidinger KA, Landsberg JHC, Tomas R, Vargo GA, editors. Harmful Algae 2002. St. Petersburg: Florida Fish and Wildlife Conservation Commission, Florida Institute of Oceanography, and Intergovernmental Oceanographic Commission of UNESCO. p. 341-343.

Montoya NG. 2019. Paralyzing shellfish toxins in the Argentine Sea: impact, trophic transfer and perspective. Mar Fish Sci. 32 (1): 47-69.

Montoya NG, Benavídez H, Carignan MO. 2008. Determinación de ácido okadaico y primera detección de pectenotoxinas asociadas a la presencia de *Dinophysi*s sp. en el litoral argentino. Inf Invest INIDEP Nº 1/2008. 15 p.

Montoya NG, Carignan MO, Carreto JI. 2018. *Alexandrium tamarense/catenella* blooms in the Southwestern Atlantic: paralytic shellfish toxin production and its trophic transference. In: Hoffmeyer MS, Sabatini ME, Brandini FP, Calliari DL, Santinelli NH, editors. Plankton ecology of the Southwestern Atlantic: from the subtropical to the subantarctic realm. Cham: Springer International Publishing. p. 453-476.

Montoya NG, Carignan MO, Mattera MB. 2020. Toxinas algales en el Mar Argentino: nuevos hallazgos, nuevos desafíos. Acta Toxicol Argent. 28 (3): 92-107.

Montoya NG, Mattera Coy MB, Carignan MO. 2015. Caracterización pigmentaria de cultivos de fitoplancton. Inf Invest INIDEP Nº 57/2015. 14 p.

Murphy J, Riley JP. 1962. A modified single solution method for the determination of phosphate in natural waters. Anal Chim Acta. 27: 31-36.

Negri R, Silva RI. 2011. Estructura de la comunidad del fitoplancton en la estación costera EPEA durante el período 2000-2010 (provincia de Buenos Aires, Argentina). Bol Soc Argent Bot. 46: 99-100.

Negri RM. 2005. INIDEP, Informe de la campaña (CC-10/2005). Marea roja-dinámica del plancton, EPEA VII/05. Mar del Plata: Biblioteca INIDEP. 4 p.

Negri RM. 2019. Series de tiempo ecológicas Costal I-EPEA I/2019. Inf Camp INIDEP Nº 16/2019. 2 p.

Nunes S, Perez GL, Latasa M, Zamanillo M, Delgado M, Ortega-Retuerta E, Marrasé C, Simó R, Estrada M. 2019. Size fractionation, chemotaxonomic groups and bio-optical properties of phytoplankton along a transect from the Mediterranean Sea to the SW Atlantic Ocean. Sci Mar. 83 (2): 87-109.

Rodríguez F, Varela M, Zapata M. 2002. Phytoplankton assemblages in the Gerlache and Bransfield straits (Antarctic Peninsula) determined by light microscopy and CHEMTAX analysis of HPLC pigment data. Deep-Sea Res II Top Stud Oceanogr. 49 (4): 723-747.

Ruiz MG. 2018. Variabilidad de las propiedades bio-ópticas en la serie de tiempo Estación

permanente de estudios Ambientales (EPEA) complementando mediciones in situ y satelitales [PhD thesis]. Mar del Plata: Facultad de Ciencias Exactas y Naturales, Universidad Nacional de Mar del Plata. 128 p.

Ruiz MG, Lutz VA, Segura V, Berghoff CF, Negri RM. 2020. The color of EPEA: variability in the in situ bio-optical properties in the period 2000-2017. Mar Fish Sci. 33 (2): 205-225.

Ruiz MG, Silva R, Martínez Goycochea A, Montoya NG. 2023. Relaciones pigmento:-clorofila *a* determinadas por CHEMTAX a partir de muestras naturales de floraciones algales de la región norte de la plataforma continental argentina. Inf Invest INIDEP Nº 72/2023. 20 p.

Sar EA, Sunesen I, Goya AB, Lavigne AS, Tapia E, Garcia C, Lagos N. 2012. First report of diarrhetic shellfish toxins in mollusks from Buenos Aires Province (Argentina) associated to *Dinophysis* spp.: evidence of Okadaic acid, Dinophysistoxin-1 and Acyl-derivatives. Bol Soc Argent Bot. 47 (1/2): 5-14.

Schlüter L, Møhlenberg F, Havskum H, Larsen S. 2000. The use of phytoplankton pigments for identifying and quantifying phytoplankton groups in coastal areas: testing the influence of light and nutrients on pigment/chlorophyll a ratios. Mar Ecol Prog Ser. 192: 49-63.

Sieburth JM, Smetacek V, Lenz JR. 1978. Pelagic ecosystem structure: heterotrophic compartments of the plankton and their relationship to plankton size fractions 1. Limnol Oceanogr. 23 (6): 1256-1263.

Silva R, Negri R, Lutz V. 2009. Summer succession of ultraphytoplankton at the EPEA coastal station (Northern Argentina). J Plankton Res. 31 (4): 447-458.

Silva RI. 2011. Dinámica del ultrafitoplancton en el Mar Argentino [PhD thesis]. Mar del Plata: Facultad de Ciencias Exactas y Naturales, Universidad Nacional de Mar del Plata. 187 p.

Simpson JH, Crisp DJ, Hearn C, Swallow JC, Currie RI, Gill AE, Simpson JH. 1981. The shelf-sea fronts: implications of their existence and behaviour. Philos Trans R Soc Ser A. 302 (1472): 531-546.

Uitz J, Claustre H, Morel A, Hooker S. 2006. Vertical distribution of phytoplankton communities in open ocean: an assessment based on surface chlorophyll. J Geophys Res C Oceans. 111 (C8): C08005. DOI: https://doi.org/10.1029/2005JC003207

Vidussi F, Claustre H, Manca BB, Luchetta A, Marty J-C. 2001. Phytoplankton pigment distribution in relation to upper thermocline circulation in the eastern Mediterranean Sea during winter. J Geophys Res C Oceans. 106 (C9): 19939-19956.

Viñas MD, Negri RM, Cepeda GD, Hernández D, Silva R, Daponte MC, Capitanio FL. 2013. Seasonal succession of zooplankton in coastal waters of the Argentine Sea (Southwest Atlantic Ocean): prevalence of classical or microbial food webs. Mar Biol Res. 9 (4): 371-382.

Zapata M, Jeffrey SW, Wright SW, Rodríguez F, Garrido JL, Clementson L. 2004. Photosynthetic pigments in 37 species (65 strains) of Haptophyta: implications for oceanography and chemotaxonomy. Mar Ecol Prog Ser. 270: 83-102.

Zapata M, Rodríguez F, Garrido JL. 2000. Separation of chlorophylls and carotenoids from marine phytoplankton: a new HPLC method using a reversed phase C8 column and pyridine-containing mobile phases. Mar Ecol Prog Ser. 195: 29-45.